

Thermoelectric transport in perfectly conducting channels in quantum spin Hall systems

Ryuji Takahashi¹ and Shuichi Murakami^{1,2}

¹*Department of Physics, Tokyo Institute of Technology, Ookayama, Meguro-ku, Tokyo 152-8551, Japan*

²*PRESTO, Japan Science and Technology Agency (JST), Kawaguchi, Saitama 332-0012, Japan*

(Received 12 March 2010; published 5 April 2010)

Thermoelectric transport of two-dimensional quantum spin Hall systems are theoretically studied in narrow ribbon geometry. We find that at high temperature electrons in the bulk states dominate. However, by lowering temperature, the “perfectly conducting” edge channels becomes dominant, and a bulk-to-edge crossover occurs. Correspondingly, by lowering temperature, the figure of merit first decreases and then will increase again due to edge-state-dominated thermoelectric transport.

DOI: [10.1103/PhysRevB.81.161302](https://doi.org/10.1103/PhysRevB.81.161302)

PACS number(s): 73.50.Lw, 71.90.+q, 72.20.Pa, 73.43.-f

Thermoelectric conversion of heat into energy is one of the challenging topics in material science. The efficiency of thermoelectric energy converters depends on the transport coefficients of the constituent materials through the figure of merit. The figure of merit ZT is defined by $ZT = \frac{\sigma S^2 T}{\kappa}$,¹ where T is the temperature, σ is the electrical conductivity, S is the Seebeck coefficient, and κ is the thermal conductivity from electrons and phonons. Maximum efficiency of a thermoelectric conversion cycle depends on ZT and the highest record of ZT is on the order of unity. It is an important but challenging issue to search for thermoelectric systems with larger ZT . There have been several proposals to overcome this conflict and to optimize the thermoelectric efficiency. One of the proposals is the phonon glass and electron crystal² (PGEC). Because the phonon carries heat but not charge, phonon conduction reduces thermoelectric efficiency. Hence to achieve a high ZT , the system should be a bad conductor for phonons but a good conductor for electrons. These two conditions often conflict with each other, making materials search difficult. Another proposal is low dimensionality.³ Low-dimensional systems have a peaked structure in the density of states, which is good for large S . Despite these proposals, good thermoelectrics have remained elusive and awaits qualitatively new approaches for improvement of ZT .

In this Rapid Communication, we propose that the quantum spin Hall (QSH) materials show enhanced thermoelectric figure of merit at low temperature. The QSH systems are new state of matters for bulk insulators,⁴⁻⁶ realized in two dimension (2D) and in three-dimension (3D). The 2D QSH system has gapless edge states which are stable against non-magnetic impurities.^{7,8} Hence we expect that in dirty systems, electron conduction through the edge states remain good, while phonon conduction is suppressed, satisfying the PGEC criterion. In addition, the edge states are one-dimensional (1D), which fits the “low-dimensional” criterion. Another good reason for this expectation is that the QSH effect was observed in $\text{Bi}_{1-x}\text{Sb}_x$,⁹ Bi_2Se_3 ,¹⁰ and Bi_2Te_3 (Ref. 11) which are good thermoelectric materials.

In 2D QSH systems in ribbon geometry, both the bulk states and edge states contribute. Because the number of bulk states is proportional to the ribbon width, we set the ribbon width to be very narrow, thereby the edge states can have comparable or even larger contribution, compared with the

bulk. We then find that the bulk and edge contributions compete each other. We also find that there occurs a bulk-to-edge crossover when the temperature is lowered. Because the edge states undergo inelastic scattering and lose their coherence, inelastic scattering length ℓ_{inel} gives an effective system size for quantum transport by edge states. As the temperature is lowered, ℓ_{inel} become longer, and the edge states become dominant in thermoelectric transport. We note that the edge transport cannot be dominant over the bulk transport at room temperature because ℓ_{inel} might become very short.

The electric current j and thermal current w are coupled, and are induced by the thermal gradient or the electric field. In a linear response, they are described as

$$\begin{pmatrix} j/q \\ w \end{pmatrix} = \begin{pmatrix} L_0 & L_1 \\ L_1 & L_2 \end{pmatrix} \begin{pmatrix} -\frac{d\mu}{dx} \\ -\frac{1}{T} \frac{dT}{dx} \end{pmatrix}, \quad (1)$$

where q is the electron charge $-e$ and μ is the chemical potential. Thermal and electric properties are given by

$$\sigma = e^2 L_0, \quad S = -\frac{1}{eT} \frac{L_1}{L_0}, \quad \kappa_e = \frac{1}{T} \frac{L_0 L_2 - L_1^2}{L_0},$$

$$ZT = \frac{L_1^2}{L_0 L_2 - L_1^2 + \kappa_L T L_0},$$

where κ_e is the electron thermal conductivity and κ_L is phonon thermal conductivity.

We first consider the edge transport only and neglect the bulk part. This corresponds to a case with very strong disorder, where the bulk states are assumed to be insulating, and the phonon heat transport is negligible. To describe the coherent transport of the edge states, we use the Landauer formula. The density of states are schematically shown in Fig. 1. The edge states are assumed to be perfectly conducting over the whole sample and the transmission coefficient $T(E)$ is unity when the electron energy is within the bulk gap ($-\Delta < E < 0$). Here we measure the energy from the bottom of the conduction band and Δ is the energy gap. To clarify an interplay between the bulk and the edge states, we focus on

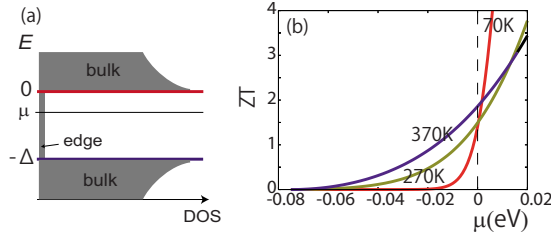


FIG. 1. (Color online) (a) Schematic bands for the bulk and edge states used in the calculation. (b) Thermoelectric figure of merit ZT as a function of chemical potential μ , by considering only the edge states in the 2D QSH system. Transport by bulk carriers and phonons is ignored.

the bottom of the bulk conduction band and neglect the valence band. We restrict the chemical potential to be $-\Delta/2 \ll \mu$. L_ν is given by

$$L_\nu^e = \frac{\ell}{sh} \int dE T(E) (E - \mu)^\nu \left(-\frac{\partial f}{\partial E} \right), \quad (2)$$

where the suffix e means the edge transport, h is the Planck constant. ℓ and s are the length of the sample and the cross section of the sample. This is rewritten as

$$L_\nu^e = \frac{2\ell}{sh} (k_B T)^\nu \int_{-\bar{\Delta}-\bar{\mu}}^{-\bar{\mu}} x^\nu \frac{e^x}{(e^x + 1)^2} dx, \quad (3)$$

where $\bar{\mu} = \frac{\mu}{k_B T}$, and $\bar{\Delta} = \frac{\Delta}{k_B T}$. We calculate ZT , by employing the gap size of Bi_2Te_3 ($\Delta = 0.15$ eV). The result (Fig. 1) shows that ZT becomes larger and well exceeds unity, when the chemical potential is in the bulk band. It is because the edge states carry large energy.

In reality, when the chemical potential is in the bulk band, the bulk transport dominates, and reduces ZT from the otherwise large value. We treat the bulk and the edge transport independently, which is valid within the inelastic scattering length. We calculate the bulk transport by the Boltzmann equation as

$$L_\nu^b = \int dE (E - \mu)^\nu \left(-\frac{\partial f}{\partial E} \right) D(E) \tau, \quad (4)$$

where the suffix b means the bulk transport and $D(E)$ is the density of states. τ is the relaxation time which is assumed to be constant. The bulk band is assumed to be parabolic with an effective mass m . For simplicity, we include only the first subband due to the confinement within the ribbon, by assuming that the gap between the first subband and second subband is large. The transport coefficients are then given by $L_\nu = L_\nu^e + L_\nu^b$ with

$$L_\nu^b = \frac{4\sqrt{2mk_B T} \mu^* c (k_B T)^\nu}{esh} \int_{-\bar{\mu}}^{\infty} \frac{\sqrt{x + \bar{\mu}} x^\nu e^x}{(e^x + 1)^2} dx \quad (5)$$

where μ^* is the mobility and the coefficient c is the number of the carrier pockets.

We calculate these transport properties at $T = 1.8$ K. We again employ the parameters for Bi_2Te_3 as follows. The parameters for bulk transport is taken from those for bulk

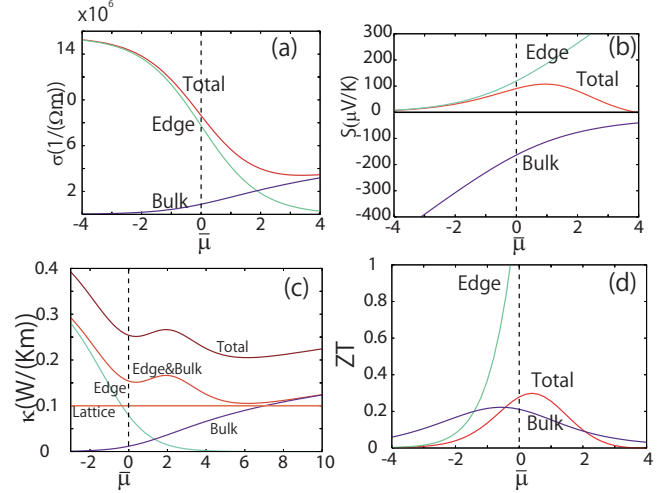


FIG. 2. (Color online) A calculation example of (a) Conductivity, (b) Seebeck coefficient, (c) thermal conductivity, and (d) ZT as a function of the chemical potential.

Bi_2Te_3 . The electron effective mass is $0.02m_e$ where m_e is the electron mass, c is 6. μ^* is measured at temperatures higher than 80 K and we estimated μ^* to be $2000 \text{ cm}^2 \text{ V}^{-1} \text{ s}^{-1}$ at $T = 1.8$ K by assuming that μ^* saturates at lower temperature due to disorder. The effective system size ℓ is the inelastic scattering length ℓ_{inel} , and we assume $\ell \sim 1 \text{ } \mu\text{m}$, which is a lower bound of ℓ_{inel} in HgTe quantum well at 1.8 K.¹⁹ s is $10 \text{ nm} \times 0.5 \text{ nm}$. κ_L is $0.1 \text{ W m}^{-1} \text{ K}^{-1}$, which is expected from extrapolation from experimental data¹² and theoretical estimate.¹³ These parameters might have some error bars because of the lack of the experimental data for Bi_2Te_3 thin film. The results are shown in Fig. 2. For these parameters the energy difference between the first and the second subbands is about 0.14 eV, and the chemical potential μ is assumed to be less than this energy. Many thermoelectric materials such as Bi_2Te_3 are narrow-gap semiconductors and the effective mass is much smaller than the electron mass. Hence the subband structure is prominent and the above assumption is satisfied without difficulty.

From Figs. 2, ZT has a maximum when the chemical potential μ is near the band edge. This results from a competition between the bulk and the edge states as follows. The Seebeck coefficient from the bulk states is larger when μ is in the bulk gap whereas that from the edge states is larger when μ is in the bulk band. Their effects tend to cancel each other because their charges have opposite signs. Therefore, maximum of ZT occurs when μ is around the band edge.

For optimization of the thermoelectric figure of merit in QSH systems, we define the following dimensionless parameters from the prefactors in Eqs. (3) and (5):

$$r = \left[\frac{2\ell}{sh} \right] / \left[\frac{4\sqrt{2mk_B T} \mu^* c}{esh} \right] = \frac{e\ell}{2\sqrt{2mk_B T} \mu^* c}, \quad (6)$$

$$g = \left[\frac{\kappa_L}{k_B^2 T} \right] / \left[\frac{4\sqrt{2mk_B T} \mu^* c}{esh} \right] = \frac{\kappa_L esh}{4\sqrt{2mk_B^5 T^3} \mu^* c}. \quad (7)$$

The parameter r represents the ratio between the edge and the bulk transport and g represents the ratio between the

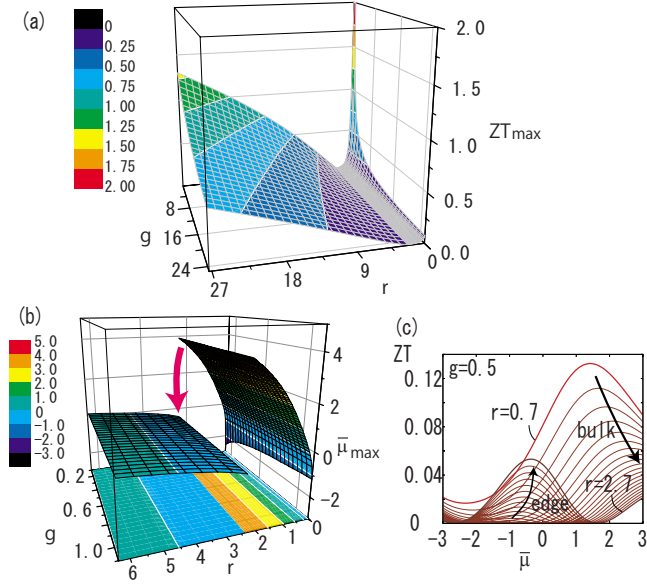


FIG. 3. (Color online) (a) ZT_{\max} and (b) $\bar{\mu}_{\max}$ as a function of r and g . (c) ZT as a function of $\bar{\mu}$ for various values of r at $g=0.5$. Bulk-to-edge crossover is seen by increasing r .

phonon heat transport and the bulk transport. These ratios characterize thermoelectric transport of 2D QSH systems. For each r and g we maximize ZT as a function of $\bar{\mu}$. In Fig. 3, we show the maximum ZT_{\max} and the value of $\bar{\mu} = \bar{\mu}_{\max}$ giving the maximum. To focus on an interplay between bulk and edge transport, we restrict μ to be near the conduction band edge, and ignore the valence band, by putting $\bar{\Delta} \rightarrow \infty$. From Fig. 3(a), as a function of r , ZT_{\max} becomes minimum at $r \sim 2.6$, because of a competition between the edge- and bulk-state transport. This interplay is prominent in the plot of $\bar{\mu}_{\max}$ in Fig. 3(b). The plot has a jump at around $r \sim 2.6$. As seen in Fig. 3(c), at about $r \sim 2.6$, the plot of ZT as a function of $\bar{\mu}$ has two peaks, one from the bulk and the other from the edge. As r passes through 2.6 from below, the peak from the edge dominates the peak from the bulk, and bulk-to-edge crossover occurs.

In Fig. 3(a) we can see that at $r=0$ (no edge transport), the resulting ZT is sensitive to g , and it is important to reduce g by suppressing the phonon heat transport. However, disorder also suppresses electronic transport and ZT is not enhanced so much. On the other hand, as r becomes larger, the result becomes insensitive to g . Disorder will enhance r , because the bulk mobility becomes smaller. The ZT will then be enhanced. Generally, at low temperatures both r and g tend to increase as T decreases, as we explain in the following. As T is lowered, the mobility μ^* increases and eventually saturates. κ_L is given by $\kappa_L = \frac{1}{3} C v_L l_L$, where C is the phonon specific heat, v_L is the phonon velocity, and l_L is the phonon mean-free path. As the temperature decreases, l_L becomes larger and saturates, while C decreases; hence, κ_L first increases and then decreases at lower temperatures. From these behaviors, r and g tend to increase at low temperatures, possibly below around 10 K. An estimation using the above-mentioned parameters for Bi_2Te_3 nanoribbon gives $r=9.4$ and $g=8.2$ at $T=1.8$ K, which is located in the edge-

dominated regime. We can estimate the crossover temperature for Bi_2Te_3 narrow ribbon taking into account the temperature dependence μ^* and κ_L in the similar way as in Fig. 2, and assuming that ℓ_{inel} decreases as $T^{-1.5}$ as has been observed in quantum Hall systems.¹⁴ The crossover temperature is estimated to be around 5–10 K.

To realize the edge-dominated transport, the ribbon width w should be much longer than the penetration depth λ of the edge states, thereby we can ignore hybridization of the gapless edge states at the opposite edges. This hybridization induces a gap $\delta \sim t e^{-w/\lambda}$ to the edge states,¹⁵ where t is the bandwidth (several eV). The penetration depth λ depends on the systems, and in some systems such as Bi ultrathin film, it is estimated to be on the order of the lattice constant.¹⁶ As we set $w=10$ nm which is several decades of the lattice constant, the hybridization gap δ is estimated to be on the order of mK. Thus in our temperature range above 1 K, this gap can be safely ignored. When we make the ribbon width to be much narrower, comparable to the penetration depth λ , the edge states at opposite edges hybridize and opens a sizable gap,¹⁵ killing the perfectly conducting edge channels.

In 2D QSH systems, elastic backscattering of edge states due to nonmagnetic impurities is prohibited.^{7,8} Inelastic scattering is a key factor to characterize transport properties of the system. The electrons in edge states keep their coherence within the inelastic scattering length ℓ_{inel} , which plays the role of the effective system size. We first estimate the electron-phonon (el-ph) inelastic scattering length ℓ_{inel} , following the calculation on the quantum Hall (QH) system.¹⁷ Here we assume the edge-state dispersion to be linear with velocity v_c . We put the bulk wave functions to be proportional to $\sin(\pi y/w)$. By considering scattering by 2D longitudinal acoustic phonons, the relaxation time τ is given by $\tau^{-1} = (\tau^{ee})^{-1} + (\tau^{eb})^{-1}$, where τ^{ee} and τ^{eb} are relaxation times by the edge-edge, the edge-bulk el-ph scattering. Following Ref. 17 we obtain

$$\frac{1}{\tau^{ee}} \sim \frac{\pi V_{ep}^2 T^2}{16 \rho c_L^3 v_c}, \quad \frac{1}{\tau^{eb}} \sim \frac{\pi^3 V_{ep}^2 T^2}{\rho c_L^3 v_c} \left(\frac{\lambda}{W} \right)^3, \quad (8)$$

where V_{ep} is a screened el-ph scattering potential. If we take $V_{ep}=10^{-19}$ J, $T=1$ K, $\rho=10^{-6}$ kg/m², $c_L=10^3$ m/s, $\lambda=10^{-10}$ m, and $W=10^{-9}$ m as an example, we get $\tau^{ee} \sim 10^{-8}$ s and $\tau^{eb} \sim 10^{-6}$ s. If $v_c \sim 10^6$ m/s and $\ell_{\text{inel}} = v_c \tau \sim 10^{-2}$ m. Experimental ℓ_{inel} is much shorter, implying that el-ph scattering is not crucial among various inelastic scattering in the QSH system around 1 K.

In addition to the el-ph interaction, the electron-electron (e-e) interaction also induces decoherence of edge states. There are two types of e-e interaction: edge-edge e-e and edge-bulk e-e interactions. The edge-edge e-e interaction is renormalized into the edge state action and form the Luttinger liquid. Therefore this edge-edge e-e interaction does not cause dephasing if the system is clean enough and the edge channels remain perfectly conducting well above Kondo temperature.¹⁸ In disordered systems, it gives rise to a finite inelastic scattering time while its estimate will be difficult. In addition, the edge-bulk e-e interaction also appears at finite temperature and it depends crucially on the details of

the system. Calculation of e-e interaction in the QSH systems is interesting but is beyond the scope of the present Rapid Communication.

The inelastic scattering length ℓ_{inel} is accessible experimentally. In the HgTe quantum well, nonlocal edge-state transport is observed¹⁹ in 1 μm sample at 1.8 K. It indicates that ℓ_{inel} is longer than the sample size, $\ell_{\text{inel}} \geq 1 \mu\text{m}$ at $T = 1.8$ K. It is limited by the potential inhomogeneity due to gating. On the other hand, the inelastic scattering length is measured in a QH system to be about 1 μm at 1 K (Ref. 14) and is decreasing function of temperature. Based on these data we have used $\ell_{\text{inel}} = 1 \mu\text{m}$ at $T = 1.8$ K in obtaining Fig. 2. If the inelastic scattering length can be made longer, it will increase r and enhance ZT by edge-dominated thermoelectric transport.

We address implications of our theory for 3D QSH systems (topological insulators). Because the surface states on 3D QSH systems are not perfectly conducting, the effect of surface states in 3D QSH systems on thermoelectricity will be less prominent than that of edge states in 2D QSH systems studied in this Rapid Communication. Nevertheless, there can be one promising possibility also in the 3D QSH systems. In 3D QSH systems, protected 1D states²⁰ of the crystal exist on line dislocations, depending on the bulk topological numbers. These 1D states are perfectly conducting. Recently, a prominent magnetofingerprint was observed in a topological insulator Bi_2Se_3 and it is suggested that the phase coherence is retained over 2 mm at around 1 K.²¹ It is also suggested²¹ that the transport involved in this magnetofingerprint is carried by these 1D states on dislocations. If this

scenario is true, they can be dominant in low temperatures, as we have shown in this Rapid Communication. The estimated phase coherence length $\ell_{\text{inel}} \sim 2$ mm is three orders of magnitude larger than that we used in our calculation and it is favorable for thermoelectric transport.

Recently, an anomalous enhancement of the Seebeck coefficient at 7 K is reported in $p\text{-Bi}_2\text{Se}_3$.²² Though our 2D model cannot describe three-dimensional $p\text{-Bi}_2\text{Se}_3$, we may attribute this enhancement to either surface states or 1D states along line dislocations. In particular, the 1D states form perfectly conducting channels and will enhance the figure of merit. We note that in our calculation the edge and bulk contributions to the Seebeck coefficient has opposite signs because the carrier charges have opposite signs (i.e., holes and electrons) and therefore the Seebeck coefficient changes sign at the bulk-to-edge crossover by changing T . On the other hand, the Seebeck coefficient on $p\text{-Bi}_2\text{Se}_3$ does not change sign by lowering temperature. Within our interpretation this implies that the bulk carriers and the 1D carriers have the same signs for the charge in the experiment.

To summarize, we study thermoelectric properties of two-dimensional quantum spin Hall systems. The edge states become dominant in thermoelectric transport at low temperature, which might be below 5–10 K for narrow ribbons. This bulk-to-edge crossover temperature is higher for longer inelastic scattering length of edge states.

We are grateful to T. Machida, X.-L. Qi, and S.-C. Zhang for helpful discussions. This research is supported in part by Grant-in-Aids from MEXT.

-
- ¹H. J. Goldsmid, *Thermoelectric Refrigeration* (Plenum, New York, 1964).
- ²G. A. Slack, in *CRC Handbook of Thermoelectrics*, edited by D. M. Rowe (CRC Press, Boca Raton, 1995), pp. 407–440.
- ³L. D. Hicks and M. S. Dresselhaus, *Phys. Rev. B* **47**, 12727 (1993); **47**, 16631 (1993).
- ⁴C. L. Kane and E. J. Mele, *Phys. Rev. Lett.* **95**, 146802 (2005); **95**, 226801 (2005).
- ⁵B. A. Bernevig and S.-C. Zhang, *Phys. Rev. Lett.* **96**, 106802 (2006).
- ⁶S. Murakami, *Phys. Rev. Lett.* **97**, 236805 (2006).
- ⁷C. Wu, B. A. Bernevig, and S.-C. Zhang, *Phys. Rev. Lett.* **96**, 106401 (2006).
- ⁸C. Xu and J. E. Moore, *Phys. Rev. B* **73**, 045322 (2006).
- ⁹D. Hsieh *et al.*, *Nature (London)* **452**, 970 (2008).
- ¹⁰Y. Xia *et al.*, *Nat. Phys.* **5**, 398 (2009).
- ¹¹Y. L. Chen *et al.*, *Science* **325**, 178 (2009).
- ¹²D. K. C. MacDonald *et al.*, *Philos. Mag.* **4**, 433 (1959).
- ¹³J. Zou and A. Balandin, *J. Appl. Phys.* **89**, 2932 (2001).
- ¹⁴T. Machida, H. Hirai, S. Komiyama, and Y. Shiraki, *Phys. Rev. B* **54**, 16860 (1996).
- ¹⁵B. Zhou, H. Z. Lu, R. L. Chu, S. Q. Shen, and Q. Niu, *Phys. Rev. Lett.* **101**, 246807 (2008).
- ¹⁶M. Wada, S. Murakami, F. Freimuth, and G. Bihlmayer (unpublished).
- ¹⁷H. L. Zhao and S. Feng, *Phys. Rev. Lett.* **70**, 4134 (1993).
- ¹⁸J. Maciejko, C. Liu, Y. Oreg, X. L. Qi, C. Wu, and S. C. Zhang, *Phys. Rev. Lett.* **102**, 256803 (2009).
- ¹⁹A. Roth *et al.*, *Science* **325**, 294 (2009).
- ²⁰Y. Ran, Y. Zhang, and A. Vishwanath, *Nat. Phys.* **5**, 298 (2009).
- ²¹J. G. Checkelsky, Y. S. Hor, M. H. Liu, D. X. Qu, R. J. Cava, and N. P. Ong, *Phys. Rev. Lett.* **103**, 246601 (2009).
- ²²Y. S. Hor, A. Richardella, P. Roushan, Y. Xia, J. G. Checkelsky, A. Yazdani, M. Z. Hasan, N. P. Ong, and R. J. Cava, *Phys. Rev. B* **79**, 195208 (2009).